Dynamics of Bimodal Growth in Pentacene Thin Films

Alex C. Mayer,[1] Alexander Kazimirov,[2] and George G. Malliaras[1,*]

[1]*Materials Science and Engineering, Cornell University, Ithaca, New York 14853, USA*
[2]*Cornell High Energy Synchrotron Source, Ithaca, New York 14853, USA*

(Received 5 May 2006; published 7 September 2006)

Previous studies have established that pentacene films deposited on silicon oxide consist of a substrate-induced ''thin-film'' phase, with the bulk phase of pentacene detected in thicker films only. We show that the bulk phase nucleates as early as the first monolayer, and continues to nucleate as film growth progresses, shadowing the growth of the thin-film phase. Moreover, we find that the transition between the ''thin-film'' and the bulk phase is not a continuous one, as observed in heteroepitaxial systems, but rather the two phases nucleate and grow independently.

DOI: 10.1103/PhysRevLett.97.105503 PACS numbers: 61.10.Kw, 61.66.Hq, 68.55.Jk, 68.55.Nq

Organic electronics, a technology that uses carbon-based semiconductors for applications that range from flat panel displays to radio frequency identification tags, is viewed as a promising compliment to silicon-based electronics [1]. One particular device that is being developed using organic semiconductors is the organic thin-film transistor (OTFT). These devices are currently receiving a great deal of attention, as their performance has reached levels comparable to that of transistors based on amorphous silicon [2]. The realization that the performance of these devices is intimately connected to the structure and morphology of the organic film has spurred numerous studies of organic semiconductor growth [3,4], and the study of these materials has revealed interesting growth physics [5–7]. Among the various materials used for OTFTs, pentacene has been established as a model system, as it readily forms polycrystalline thin films with a hole mobility among the highest reported for an organic semiconductor [2,8].

Organic semiconductor crystals are known to exhibit polymorphism, and their films often exhibit substrate-induced crystalline phases [9,10]. For example, the crystalline structure of vacuum deposited pentacene films is known to differ from that of bulk pentacene crystals grown near equilibrium from solution or vapor [11–13]. The substrate-induced structure has been referred to as the ''thin-film'' phase in the literature and it is characterized by an expansion in the d_{001} spacing between layers that is 15.4 Å [11,12], as compared with the bulk phase (the most prevalent polymorph), which has a d_{001} spacing on the order of 14.5 Å [13]. The crystalline structure of this thin-film phase has been recently solved using synchrotron x-ray diffraction [14,15], and electron diffraction [16,17].

Specular x-ray diffraction in thicker films reveals the presence of the bulk phase [12,15,18,19]. However, its evolution, and the nature of its coexistence with the thin-film phase has only been explored thermodynamically [17]. It is not known, for example, at which thickness the first bulk crystallites are first nucleated or how the two phases evolve after the initial bulk nucleation. Several studies seem to suggest that initially pentacene grows in the thin-film phase until some critical thickness is reached after which the bulk phase nucleates [12,15–20]. On the other hand, it could also be that the bulk phase nucleates at the substrate and evolves in coexistence with the thin-film phase but at such a small fraction that it remains undetectable by conventional methods until a certain thickness is reached. Moreover, the exact mechanism involved in this transition from the thin-film phase to the bulk phase is still unknown. Is, for example, the thin-film phase a strained metaphase which is induced by the substrate and is gradually converted to the bulk phase over several unit cells, as is the case in heteroepitaxial growth [21]?

To answer these questions, we combined several x-ray diffraction techniques to monitor the evolution of the two phases. Pentacene films were prepared in a custom made vacuum chamber (Advanced Design Consulting, Inc.), which was mounted in a four circle diffractometer at the A2 station of the Cornell High Energy Synchrotron Source (CHESS). The substrates consisted of silicon wafers with a 3000 Å thermal oxide grown at the Cornell Nanoscale Facility. The substrates were cleaned prior to deposition in an ultrasonic bath with deionized water; dried with filtered, dried nitrogen; and given a UV/O_3 treatment. Pentacene films were thermally deposited in high vacuum ($< 10^{-6}$ Torr) at a deposition rate of approximately 4 Å/min. The substrate was held at 60 °C in order to accelerate the appearance of the bulk phase, which is known to be more prevalent in films grown at elevated substrate temperatures [18]. The deposition was monitored by a quartz-crystal microbalance, which was passivated with pentacene and was calibrated using atomic force microscopy measurements in sub-ML thick films grown on room temperature SiO_2.

Diffraction experiments were performed during film deposition at CHESS using 10.05 keV x-rays with a flux of $\sim 10^{13}$ photons/sec, incident on the sample through a Be window and using a scintillator counter to measure the scattered x-ray intensity. θ–2θ scans for the (002) peaks of the thin-film and bulk phases were taken during the depo-

sition. Each scan took between 65 and 90 sec. After deposition grazing-incidence x-ray diffraction (GIXD) was performed as described in a previous publication [15]. 2D x-ray diffraction was performed on a Bruker-AXS General Area Detector Diffraction System. No post-deposition changes in structure were observed in films kept inside the growth chamber at the growth temperature or below.

The *real-time* evolution of a pentacene film was monitored by scanning the (002) peaks for both the thin-film and the bulk phases, at the rate of four scans per monolayer. The (002) peaks were chosen due to their large separation, as well as due to the good signal-to-noise ratio they afford. The thin-film peak, centered around $q = 0.82$ Å^{-1}, was resolved with a good signal-to-noise ratio after a thickness of 200 Å. On the other hand, the bulk phase peak, centered around $q = 0.88$ Å^{-1} was resolved only after 600 Å, in agreement with previous studies [12,15,17–19]. General area x-ray diffraction results from one of these films (not shown here) show that the (002) reflections are along the specular direction. Therefore the thin-film and the bulk crystallites are aligned with their c^* axis perpendicular to the substrate, without any mosaicity.

Figure 1(a) shows the evolution of the average thickness of the thin-film and the bulk phases, h_{TF} and h_B, respectively, as a function of total film thickness. These quantities were obtained from the width of the (002) peaks using the Scherrer equation [22,23]. The dashed line in Fig. 1(a) represents the limit where the bulk phase is never nucleated and the film consists entirely of the thin-film phase. The experimental data for h_{TF} track this limit up to a thickness of 400 Å, beyond which a noticeable deviation occurs and the thin-film phase tends towards saturation. At the end of the deposition, h_{TF} is equal to at 635 Å, approximately half of the total film thickness. Surprisingly, h_B does not make up for the difference; as it is about 380 Å at the end of the run. The reason for this is discussed below.

Additional information on the evolution of the two phases can be obtained from the integrated intensity of the (002) peaks. The integrated intensity of a reflection is a function of the size of the crystalline domains and their electron density [22]. Given that the volumes of the unit cells of the thin-film and bulk phases are approximately equal [15], their electron densities should also be equal. Therefore, the quantities V_{TF} and V_B defined as

$$V_{TF,B} = \sqrt{\int I_{TF,B} dq_z} \qquad (1)$$

reflect the total number of unit cells of the thin-film and the bulk phases, respectively. In the above equation, I_{TF} and I_B are the intensities of the thin-film and the bulk (002) peaks, respectively.

The thickness evolution of V_{TF} and V_B is shown in Fig. 1(b). V_{TF} shows a similar thickness dependence as

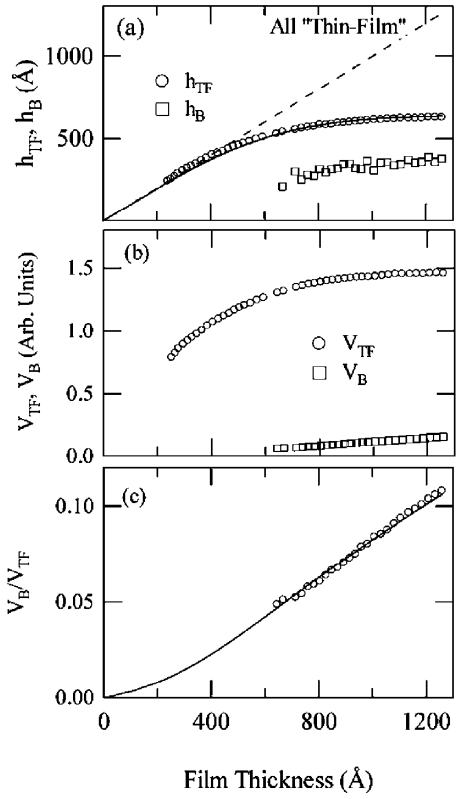

FIG. 1. Dependence on the total film thickness of (a) the average thickness of the thin-film and the bulk phases, (b) the square root of the integrated intensities of the peaks that corresponds to these two phases, and (c) the ratio of these values. The dashed line represents the limit where no bulk phase is nucleated, while the solid lines are fits.

the thickness of the thin-film phase [see Fig. 1(a)]. This is expected, as the thin-film crystallites are in phase with each other and scatter in phase in the specular direction. Therefore, V_{TF} reflects the volume of the thin-film phase, which is proportional to the thickness of the thin-film phase h_{TF}. V_B, on the other hand, is considerably smaller than V_{TF}, and its magnitude cannot account for the saturation in the latter. The bulk crystallites must, therefore, not be scattering in phase in the specular direction.

The lack of in-phase scattering from the bulk crystallites can be explained by a simple model according to which the film is initially composed of the thin-film phase until time $t = t_0$ ($t_0 \geq 0$), when bulk crystallites begin to nucleate at a constant nucleation rate. The exaggerated cartoon in the inset of Fig. 2 shows a film that contains a bulk crystallite that nucleated on the substrate and another one that nucleated on the second monolayer. Once nucleated, a bulk crystallite will grow laterally by capture of pentacene molecules that land on exposed "thin-film" phase terraces and diffuse over to that crystallite. Keeping in line with a distributed growth model, the rate of capture will be proportional to the crystallite perimeter [24]. The evolution of a bulk crystallite after nucleation is then described by

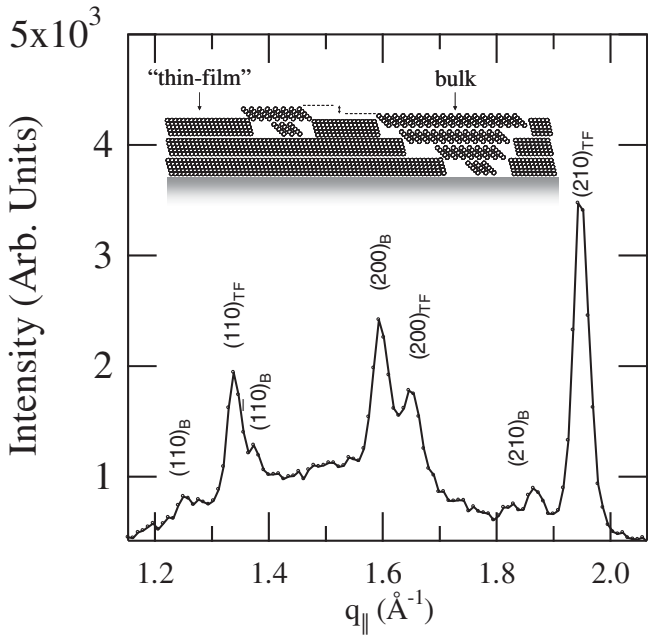

FIG. 2. GIXD from a 3000 Å pentacene film displaying the in-plane peaks for both phases. For experimental conditions see Ref. [15]. The inset shows a cartoon of the model, where bulk crystallites are nucleated on the substrate and on the second monolayer. The arrow between the dotted lines shows the height difference between the two bulk crystallites.

$$\frac{d\theta_{B,i}(t)}{dt} = \nu\alpha d_{B,i}(t)\left(1 - \sum_{j\neq i}\theta_{B,j}(t)\right), \tag{2}$$

where $\theta_{B,i}(t)$ is the coverage of crystallite i at time t, ν is the deposition rate, α represents the rate at which molecules add to the crystallite, and $d_{B,i}(t)$ is the crystallite perimeter. For compact crystallites, $d_B(t) = \sqrt{\theta_B(t)}$ [24]. The term in the parenthesis accounts for molecules that land on the top of the exposed thin-film phase.

According to this model, the thickness of the thin-film phase will grow by addition of molecules that land on thin-film phase crystallites and avoid capture by bulk crystallites. Therefore, the rate of the thin-film growth can be described by

$$\frac{dh_{\mathrm{TF}}(t)}{dt} = \nu\left(1 - \sum_{j}\theta_{B,j}(t)\right) - \sum_{j}\frac{d\theta_{B,j}(t)}{dt}, \tag{3}$$

where the right-hand side of the above equation accounts for molecules that escape capture by the bulk crystallites, while the second term represents molecules that do not [see Eq. (2)].

As bulk crystallites are nucleated at different "heights" from the substrate, and since the d_{001}-spacings of the thin-film and the bulk phases are not equal, different bulk crystallites will not scatter in phase in the specular direction (see arrow between dotted lines in inset of Fig. 2). Therefore, the ratio V_B/V_{TF} [Fig. 1(c)] is given by

$$\frac{V_B}{V_{\mathrm{TF}}} = \frac{\sum_j N_{B,j} e^{ijq\nu\tau_j}}{N_{\mathrm{TF}}}, \tag{4}$$

where N_{TF} is the number of unit cells arranged in the thin-film phase, $N_{B,j}$ is the number of unit cells in the bulk crystallite j, q is the momentum transfer, ν the deposition rate, and τ_j is the time at which the bulk crystallite j was nucleated. It should be noted that Eq. (4) is not sensitive to individual crystallite morphology, but only to the total number of unit cells in each crystallite and its distance from the substrate.

A simultaneous fit of the thin-film phase thickness data to Eqs. (2) and (3) as well as of the V_B/V_{TF} ratio to Eq. (4) is represented by the solid curves in Figs. 1(a) and 1(c), respectively. The best fit was obtained for $t_0 \sim 0$, indicating that the first bulk crystallite is nucleated on the substrate. Therefore, there is no critical thickness of the thin-film phase before the bulk phase is nucleated, and the reason why the bulk phase has remained undetected in ultrathin films is because x-ray diffraction techniques cannot discriminate such small volumes, especially when they do not scatter in phase.

According to the model above, the thin-film phase evolves as a slab at early stages. As a result, its average thickness and total volume are proportional to each other, as shown in Fig. 1. On the other hand, the functional form of h_B on the total number of molecules arranged in the bulk phase depends on the shape of the bulk crystallites. Therefore, h_B shown in Fig. 1(a) does not account for the difference between h_{TF} and the total film thickness.

The model above assumes that the bulk phase nucleates on top of the thin-film phase and that only these two phases exist in the film. This is contrary to the case of heteroepitaxy, where a substrate-induced phase evolves in a continuous way into the bulk phase over a thickness of several monolayers. For example, the first GIXD experiments that probed the growth of Al on GaAs [001], found that the position of the Al (220) peak deviated from that of bulk aluminum for the first several monolayers [21]. However, with increasing film thickness, the Al (220) peak shifted towards the bulk value. This was attributed to gradual relaxation of strain, induced by the 1% mismatch in the lattice parameters between film and substrate. For thicker aluminum films (> 1000 monolayers), only the bulk (220) peak was seen. It should be noted that GIXD is much more sensitive to such effects than specular diffraction, as it probes lattice spacing parallel to the substrate [21].

GIXD data from a pentacene film (Fig. 2) reveal a sharp contrast with the case of heteroepitaxial growth. The peaks corresponding to the thin-film phase are present in the exact same positions as previously reported [14,15]. In addition, several peaks associated with the bulk phase are visible. Since the a-b plane is parallel to the substrate in pentacene films, the positions of the crystal truncation rods can be found by solving for the reciprocal-lattice vector,

$\mathbf{G}_{hk0}$, and then taking the magnitude of the component parallel to the substrate [22,25]. The bulk phase peaks, indexed in Fig. 2, are in perfect agreement with what is expected from the bulk crystal structure [13].

The fact that there are no intermediate GIXD peaks supports the idea that bulk crystallites nucleate on top of the thin-film phase rather than evolve from it gradually over several lattice spacings. Accordingly, the structure of pentacene films evolves in the following manner: Adsorbed pentacene molecules on top of a thin-film terrace nucleate and give rise to the next thin-film layer. However, given the small difference between the cohesive energy of the thin-film and the bulk phases [26], there is always a finite probability that the latter will nucleate instead. Once a bulk nucleus is formed it will continue to grow as a bulk phase crystallite and will "shadow" the thin-film phase underneath, which causes the saturation in the thin-film phase thickness. Progressively, by means of continuous nucleation, bulk crystallites will take over the thin-film phase as the film gets thicker. This mechanism of structural evolution relies on the small differences of the cohesive energies of the bulk and thin-film phases, which are a consequence of the weak bonding in organics. As a result, this mechanism is expected to be quite generic and at work in other organic semiconductor films. The presence of two phases in an organic film will create structural defects, such as voids, which are detrimental to charge transport. This might be the reason why the field effect mobility in thin-film transistors is lower than that measured in transistors made from single crystals [27].

In conclusion, we showed that the bulk phase of pentacene thin films nucleates as early as the first monolayer, much earlier than what can be directly detected with x-ray diffraction. The bulk phase continues to nucleate as film growth progresses, shadowing the underlying thin-film phase. Moreover, we found that the transition between the thin-film and the bulk phase is not a continuous one, but rather the two phases nucleate and grow independently. The conclusions are expected to hold in other organic semiconductors too.

The authors would like to thank Jack Blakely and Randy Headrick for fruitful discussions. This work was supported by the CCMR (NSF No. DMR 96-32275). A portion of this work was conducted at CHESS (NSF No. DMR 97-13424), and at CNF (NSF No. ECS 97-31293).

*To whom all correspondence should be addressed.
Electronic address: ggm1@cornell.edu

[1] G. G. Malliaras and R. H. Friend, Phys. Today **58**, No. 5, 53 (2005).
[2] C. D. Dimitrakopoulos and P. R. L. Malenfant, Adv. Mater. **14**, 99 (2002).
[3] R. Ruiz, D. Choudhary, B. Nickel, T. Toccoli, K. C. Chang, A. C. Mayer, P. Clancy, J. M. Blakely, R. L. Headrick, S. Iannotta, and G. G. Malliaras, Chem. Mater. **16**, 4497 (2004).
[4] F. Schreiber, Phys. Status Solidi A **201**, 1037 (2004).
[5] S. Kowarik, A. Gerlach, S. Sellner, F. Schreiber, L. Cavalcanti, and O. Konovalov, Phys. Rev. Lett. **96**, 125504 (2006).
[6] R. Ruiz, B. Nickel, N. Koch, L. C. Feldman, R. F. Haglund, Jr., A. Kahn, F. Family, and G. Scoles, Phys. Rev. Lett. **91**, 136102 (2003).
[7] A. C. Mayer, R. Ruiz, H. Zhou, R. L. Headrick, A. Kazimirov, and G. G. Malliaras, Phys. Rev. B **73**, 205307 (2006).
[8] Y. Y. Lin, D. J. Gundlach, S. F. Nelson, and T. N. Jackson, IEEE Electron Device Lett. **18**, 606 (1997).
[9] B. Servet, G. Horowitz, S. Ties, O. Lagorsee, P. Alnot, A. Yassar, F. Deloffre, P. Srivastava, R. Hajlaoui, P. Lang, and F. Garnier, Chem. Mater. **6**, 1809 (1994).
[10] R. Resel, Thin Solid Films **433**, 1 (2003).
[11] T. Minakata, H. Imani, M. Ozaki, and K. Saco, J. Appl. Phys. **72**, 5220 (1992).
[12] C. D. Dimitrakopoulos, A. R. Brown, and A. J. Pomp, J. Appl. Phys. **80**, 2501 (1996).
[13] R. B. Campbell, J. M. Robertson, and J. Trotter, Acta Crystallogr. **15**, 289 (1962).
[14] S. E. Fritz, S. M. Martin, C. D. Frisbie, M. D. Ward, and M. F. Toney, J. Am. Chem. Soc. **126**, 4084 (2004).
[15] R. Ruiz, A. C. Mayer, G. G. Malliaras, B. Nickel, G. Scoles, A. Kazimirov, H. Kim, R. L. Headrick, and Z. Islam, Appl. Phys. Lett. **85**, 4926 (2004).
[16] J. S. Wu and J. C. H. Spence, J. Appl. Crystallogr. **37**, 78 (2004).
[17] L. F. Drummy and D. C. Martin, Adv. Mater. **17**, 903 (2005).
[18] I. P. M. Bouchoms, W. A. Schoonveld, J. Vrijmoeth, and T. M. Klapwijk, Synth. Met. **104**, 175 (1999).
[19] M. Shtein, J. Mapel, J. B. Benziger, and S. R. Forrest, Appl. Phys. Lett. **81**, 268 (2002).
[20] R. Ruiz, A. Papadimitratos, A. C. Mayer, and G. G. Malliaras, Adv. Mater. **17**, 1795 (2005).
[21] W. C. Marra, P. Eisenberger, and A. Y. Cho, J. Appl. Phys. **50**, 6927 (1979).
[22] B. E. Warren, *X-Ray Diffraction* (Addison-Wesley, Reading, MA, 1969).
[23] The Scherrer equation in reciprocal space is given by $(\delta q)^2 = (\delta_{\mathrm{res}})^2 + (\frac{1.8\pi}{h_{\mathrm{TF}}})^2$, where δq is the full width at half maximum of the peak (extracted by fitting a Lorentzian to the experimental data), and δ_{res} is the resolution of the detector.
[24] P. I. Cohen, G. S. Petrich, P. R. Pukite, G. J. Whaley, and A. S. Arrott, Surf. Sci. **216**, 222 (1989).
[25] The magnitude of the parallel component of the reciprocal-lattice vector $(h, k, 0)$ is given by $|\mathbf{G}_{hk0,\parallel}| = \sqrt{\frac{b^2h^2 + a^2k^2 - 2abhk\cos\gamma}{a^2b^2\sin^2\gamma}}$, where a and b are the in-plane lattice vectors and γ is the angle between them.
[26] R. G. Della Valle, E. Venuti, A. Brillante, and A. Girlando, J. Chem. Phys. **118**, 807 (2003).
[27] V. Podzorov, E. Menard, A. Borissov, V. Kiryukhin, J. A. Rogers, and M. E. Gershenson, Phys. Rev. Lett. **93**, 086602 (2004).